



RESEARCH ARTICLE

Utilizing chitosan and titanium dioxide nanomaterials and their nanocomposites for improving the growth and biochemical responses of *Sorghum bicolor* (L.)

Neelam Rani¹, Kusum Kumari¹ & Vinita Hooda^{1*}

¹Department of Botany, Maharshi Dayanand University, Rohtak (124001), India

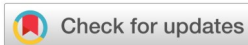
*Email: vinitahooda@yahoo.co.in

OPEN ACCESS

ARTICLE HISTORY

Received: 03 September 2023
Accepted: 16 February 2024

Available online
Version 1.0 : 05 May 2024



Additional information

Peer review: Publisher thanks Sectional Editor and the other anonymous reviewers for their contribution to the peer review of this work.

Reprints & permissions information is available at https://horizonpublishing.com/journals/index.php/PST/open_access_policy

Publisher's Note: Horizon e-Publishing Group remains neutral with regard to jurisdictional claims in published maps and institutional affiliations.

Indexing: Plant Science Today, published by Horizon e-Publishing Group, is covered by Scopus, Web of Science, BIOSIS Previews, Clarivate Analytics, NASS, UGC Care, etc. See https://horizonpublishing.com/journals/index.php/PST/indexing_abstracting

Copyright: © The Author(s). This is an open-access article distributed under the terms of the Creative Commons Attribution License, which permits unrestricted use, distribution and reproduction in any medium, provided the original author and source are credited (<https://creativecommons.org/licenses/by/4.0/>)

CITE THIS ARTICLE

Rani N, Kumari K, Hooda V. Utilizing chitosan and titanium dioxide nanomaterials and their nanocomposites for improving the growth and biochemical responses of *Sorghum bicolor* (L.). Plant Science Today (Early Access). <https://doi.org/10.14719/pst.2921>

Abstract

It is imperative to comprehensively assess the impact of nano-based technologies on plants and ensure their safety before integrating them into agricultural practices. In this context, the present study demonstrates the effect of nanosized chitosan (CS), titanium dioxide (TiO₂), and CS/TiO₂ nanocomposites (NCPs) on *Sorghum bicolor* (L.) Moench, the fifth most important grain crop globally. The nanomaterials were chemically synthesized and characterized in terms of size, surface morphology, structure, functional groups, and hydrodynamic diameter. *S. bicolor* plants were cultivated in soil spiked with these nanomaterials at two different concentrations (100 and 200 ppm) for up to 30 days. Compared to control plants, all three nanomaterials stimulated the growth of *S. bicolor* by 3-23% and enhanced nutrient uptake. Additionally, they increased the concentrations of chlorophyll (35-94%), starch (13-19%), cellulose (12-56%), and protein (3-119%) in the shoots, while reducing the malondialdehyde (MDA) content. However, elevated MDA levels in the roots of plants treated with TiO₂ nanoparticles and CS/TiO₂ NCPs indicated that mild oxidative stress had occurred, which the plant managed to counteract by enhancing antioxidant enzyme activities. The findings of this study confirm the safety of using these nanomaterials and provide a foundation for future research aimed at enhancing the growth, adaptability, and yield of *S. bicolor*.

Keywords

nanoparticles; nanocomposites; soil; jwar; antioxidant enzymes

Introduction

The paramount challenge in today's context is ensuring the food security of the rapidly growing global population. Factors such as rising temperatures, erratic rainfalls, natural disasters, nutrient-poor soil, and pest infestation, coupled with conventional farming methods, adversely affect the yield of economically significant crops (1). Hence, it is critical to explore alternative strategies that can boost agricultural productivity. This necessitates rigorous research and the adoption of emerging technologies, such as nanotechnology, to develop viable solutions.

Nanotechnology has the potential to revolutionize the agricultural system, making it more resilient while also ensuring food security in the near future. Consequently, nanoparticles (NPs) are gaining popularity as a cutting-edge material with the potential to transform current agricultural operations. Various nanoparticle-based sensors, fertilizers, and pesticide formulations have been successfully synthesized and used for plant and soil health management (2). However, to fully exploit nanotechnology in agriculture, it is crucial to develop a comprehensive understanding of plant-

nanoparticle (NP) interactions and ensure their safe use. The effect of NPs on plants varies depending on their size, shape, exposure duration, and concentration. Furthermore, it is now widely acknowledged that the effects of NPs are also plant species-specific. A particular type of NP may stimulate the growth of one plant species and inhibit the growth of another, even if all other variables remain constant. Nanomaterials can have various effects on plants, ranging from positive to neutral to harmful, without following any clear pattern. This variability in plant-NP interactions has intrigued the scientific community, highlighting the need for preliminary research on every NP-plant combination before the broader application of advanced nanotechnologies in agriculture (3-5).

Sorghum bicolor (L.) Moench, commonly known as jwar, millo, sweet sorghum, and durra, is the world's fifth most significant grain crop and serves as a promising biofuel feedstock adapted to drylands. In addition to being a vital food source for humans, it is also cultivated as forage, providing fodder for cattle and thereby addressing the food-versus-fuel dilemma favorably. However, its yield has been severely affected by various climatic factors and environmental constraints over the years. Global production decreased to 62 million tons in 2020 from 64.58 million tons in 2008, while its production in India dropped to 4.7 million tons in 2020 from 7.4 million tons in 2008 (6). Simulation studies on the impact of climate change on sorghum production in India have indicated that yields are likely to decline by 11% in 2050 and by 32% in 2080 (7). Several attempts have been made to enhance the growth and yield of sorghum through the use of nanomaterials and other nanotechnology-based interventions. The stimulatory effects of zinc oxide and copper oxide NPs at 750 mg kg⁻¹ and of silver NPs at 750, 1000, and 1250 mg kg⁻¹ on the shoot and root length of *S. bicolor*, were reported by Maity et al. (8). Cerium NPs at 10 mg L⁻¹ have been shown to alleviate drought stress by reducing oxidative damage and increasing carbon assimilation rates in *S. bicolor* (9).

In this context, the use of chitosan (CS) and titanium dioxide (TiO₂) NPs presents numerous opportunities and possibilities. While the application of CS NPs to various plant species has shown promising results, its effect on sorghum has yet to be investigated. Chitosan, a natural biopolymer derived from crustaceans and the fungal cell wall, consists of β-1,4-glucosamine and β-1,4-N-acetyl glucosamine residues connected by glycosidic bonds. Its polycationic nature contributes to its bioactivity, serving functions such as antimicrobial activity, enhancement of plant growth, increased production of secondary metabolites, and influence on photosynthesis and enzyme activities (4). For instance, CS NPs have positively affected the shoot length, number of leaves, and mineral content in finger millet at 0.1% foliar application (5). TiO₂ NPs, known for their photocatalytic properties, have been found to boost the growth of various plant species by enhancing their photosynthetic capacity (10). Lei et al. (11) reported that TiO₂ NPs improved the activity of rubisco and other antioxidant enzymes, increased chlorophyll content, and enhanced the

photosynthetic rate, leading to a higher yield in spinach. Similarly, broad bean plants treated with TiO₂ NPs exhibited better growth, with increased levels of soluble sugar, amino acids, and proline (12), alongside improved antioxidant potential and reduced levels of hydrogen peroxide (H₂O₂) and malondialdehyde (MDA).

Although few studies have reported the positive effects of TiO₂ NPs on sorghum plants, including stimulatory effects on shoot length at 1250 mg kg⁻¹ and improvements in growth parameters, chlorophyll content, and antioxidant enzyme activities with dye-coated TiO₂ NPs at 500 ppm (8, 13), these experiments often involved surface-modified TiO₂ NPs or used excessive amounts, leading to potential environmental contamination. There has been no effort to evaluate the effects of unmodified TiO₂ NPs on sorghum at lower concentrations, which is significant considering the average geogenic background of TiO₂ in soils is about 0.5%, a factor relevant to environmental safety (14).

Recently, TiO₂NPs have been used as nanofillers to reinforce the CS polymeric matrix and develop nanocomposites (NCPs) with improved mechanical, thermal, and antioxidant properties. Diverse successful applications of CS/TiO₂ NCPs in the environmental, food, and medicine sectors, such as the removal of dye, purification of water (15), as an antimicrobial agent (16), coatings for food preservation (17), drug delivery, and implant coatings (18), have been reported. Their widespread application in other fields has drawn unequivocal attention to the possibility of their use in the agriculture sector too. However, there is not even a single report on their effects on plant growth and development.

Hence, it may be interesting to report if CS and TiO₂ NPs and CS/TiO₂ NCPs can be used as growth enhancers for *S. bicolor*. To achieve this, these nanomaterials were chemically synthesized, characterized, and applied to the soil at two different concentrations, viz., 100 and 200 ppm. The impact of such nanomaterials on the growth, nutrient status, chlorophyll, protein, starch, and cellulose contents of *S. bicolor* was evaluated. The antioxidant status of plants was also measured by investigating membrane damage and the activities of antioxidant enzymes.

Materials and Methods

Chemicals

All the utilized chemicals were of analytical grade and supplied by Hi-Media Laboratories Pvt. Ltd., Mumbai; Sigma-Aldrich Chemicals Pvt. Ltd., Mumbai; Moly Chem, Mumbai; Merck Life Science Pvt. Ltd., Mumbai; Bengal Chemicals & Pharmaceuticals Ltd., Mumbai; Thomas Baker Chemicals Pvt. Ltd., Mumbai and Loba Chemie Pvt. Ltd., Mumbai. Seeds of *S. bicolor*, genotype SSG 59-3 were procured from Chaudhary Charan Singh (CCS) Haryana Agricultural University, Hisar, Haryana, India.

Synthesis of NPs and NCPs

CS (0.25 g) was dissolved in 50 mL of 2% acetic acid under stirring conditions (Tarsons, SPINOT DIGITAL-MC02, India)

followed by sonication (Q-Sonica, Q125, USA) for 15 min. Then, 20% sodium sulphate (Na_2SO_4) was added dropwise to the aqueous CS solution under the same condition and sonicated again for 15 min. The solution was left undisturbed for 2 h and centrifuged (Plasto Crafts, Rota 4R-V/F_M, India) at 5009 $\times g$ to collect the CS NPs (19).

TiO_2 NPs were synthesized by the protocol of Ghows and Entezari (20). Distilled water (50 mL) was mixed with glacial acetic acid (0.2 mL) and sonicated for 10 min. Further, 5 mL of ethanol and 2 mL of titanium tetraisopropoxide were added dropwise and then sonicated for 3h. The precipitates formed were recovered by centrifugation (17608 $\times g$ for 20 min at 25 °C) and repeatedly washed with distilled water and ethanol. The precipitates were dried for 6 h at 40 °C in a hot air oven (MAC, Macro Scientific Works, India) to obtain TiO_2 NPs.

To prepare CS/ TiO_2 NCPs, 1 g of TiO_2 NPs was dispersed in 100 mL of 1% acetic acid. This was combined with 1 g of bulk CS and sonicated for 30 min while being continuously stirred to obtain a clear solution. Then sodium hydroxide (NaOH) solution (1 M) was added dropwise until the solution attained a pH of 10. The precipitate was heated for 5 h at 80 °C, filtered, and thoroughly washed with water. After washing, it was dried overnight in a hot air oven at 60 °C (16). Sonication was carried out at 25 °C and 20 kHz (125 W, 70% amplitude) for all the experiments.

Characterization of NPs and NCPs

The synthesized particles were characterized by transmission electron microscopy (TEM, Hitachi: H-7500, 120 kV), field-emission scanning electron microscopy (FESEM, Hitachi: SU8010 Series), and X-ray diffraction (XRD, Panalytical's X'Pert Pro) techniques at Punjab University, Chandigarh. Fourier transform infrared spectroscopy (FTIR, Bruker Alphall) and zetasizer (Malvern Panalytical) analysis were performed at the Central Instrumentation Laboratory, Maharshi Dayanand University, Rohtak.

Experimental design

The *S. bicolor* plants were grown in earthen pots filled with NPs/NCPs spiked soil. The control plants (without NPs/NCPs) were also raised in parallel under the same conditions. The unspiked soil samples were analyzed for the level of nutrients and other chemical properties by an ICP spectrophotometer (ICAP 6000 Series, Thermo Scientific) at the Soil and Water Analysis Laboratory, Krishi Vigyan Kendra, Rohtak.

To create a total of 6 treatment groups, the requisite concentrations (100 or 200 ppm) of CS or TiO_2 NPs, or their NCPs were added separately to each pot holding ~5 kg of soil. A total of 5 pots (replicates) of each treatment group were raised. Each pot contains 5 seeds, thus making a total of 25 plants/group.

The concentrations of NPs were selected after a thorough literature review, wherein several studies demonstrated that CS and TiO_2 NPs had stimulatory effects on plants at concentrations between 30-200 ppm, whereas higher quantities were reported to be hazardous

and inhibit plant growth (21-24). After sterilization with 0.1% mercuric chloride for 2 min, *S. bicolor* seeds were thoroughly washed with distilled water after 2 min of sterilization with 0.1% mercuric chloride. Then, the seeds were hydroprimed for 6 h and germinated for 48 h at 30 °C in an incubator. Plants were transferred further to pots containing soil and observed for 30 days. The pots were kept in the open experimental area, receiving a photosynthetic photon flux density of approximately 1480 to 1850 $\mu\text{mol}/\text{m}^2/\text{s}$ under a bright sunny day in May (13 h light and 11 h dark period). The plants were irrigated with tap water, whenever required. On the 30th day, the control and treated plants were harvested separately, and the length, freshness, and dry weight of the shoot and root were measured. Moreover, chlorophyll, protein, starch, and cellulose contents, lipid peroxidation, and the activities of antioxidant enzymes were also investigated. Statistical analysis was performed on data obtained from five replicates of each experimental group ($n = 5$).

Determination of nutrient uptake

Nutrient uptake, such as nitrogen (N), phosphorous (P), potassium (K), and magnesium (Mg), by the control and treated *S. bicolor* plants was compared. The shoots and roots of the collected plant samples were oven dried for 48 h at 80 °C. The powdered samples were spread on carbon stubs and coated with Au with the help of a sputter coater. The elemental analysis of the dried samples was done using energy dispersive X-ray (EDX; Hitachi, SU8010 Series) at the sophisticated analytical instrumentation facility, Punjab University, Chandigarh. The samples were exposed to X-rays, and the emissions were captured by an energy-dispersive detector. The comparison of the resulting spectrum with predefined standards allowed for the precise determination of the elemental composition of the sample.

Total chlorophyll and protein content

The total chlorophyll content of the *S. bicolor* shoots was measured as described by Thakur et al. (25). Briefly, 0.5 g of the plant sample (both leaf and stem) was crushed in 80% acetone and centrifuged at 5009 $\times g$ for 20 min. The sample absorbance was taken at 643 and 663 nm. The chlorophyll content was calculated using equation (i) and the results were expressed as mg g⁻¹ of the shoot.

$$\text{Total chlorophyll} = \frac{(20.2 \times (A_{645}) + 8.02 \times (A_{663})) \times V}{1000 \times W} \quad \dots \dots \dots \text{(i)}$$

Where, V = volume of acetone used, and W = amount of the sample taken.

The content of protein in the shoot and root samples was estimated by the Bradford assay (26) and expressed as mg g⁻¹ of fresh plant material.

Starch and cellulose content

The dried material (0.1 g) was dissolved in 10 mL of hot ethanol (80%) to remove all sugars. Next, 6.5 mL of perchloric acid (52%) was added to convert the starch into glucose units (27). The amount of glucose units was estimated using the phenol method. For cellulose content estimation, 0.1 g of the sample was digested in 6 mL of

nitric acid (28). This digestion process eliminated all sugars except cellulose, which was then quantified by the anthrone assay. A glucose standard curve (10-100 g mL⁻¹) was utilized to quantify starch and cellulose, with the results represented as mg g⁻¹ of plant extract.

Lipid peroxidation

MDA was utilized as a marker of lipid peroxidation. The method employed by Thakur et al. (25) was followed to measure plant lipid peroxidation. The MDA values were expressed as µM MDA g⁻¹ of fresh weight.

Antioxidant enzymes

In the present study, we measured the effect of CS and TiO₂ NPs and CS/TiO₂ NCPs on the activities of four antioxidant enzymes, namely superoxide dismutase (SOD), catalase (CAT), ascorbate peroxidase (APx), and glutathione peroxidase (GPx). To prepare plant extracts, plant tissue (0.5 g) was ground with 5 mL of potassium phosphate buffer (0.1 M, pH 7.0). The homogenate was then centrifuged at 4 °C, 17608 ×g for 10 min. The resulting supernatant was used as an enzyme source for further investigations. In the reaction mixture of the control plants, the plant extract was replaced with equal volumes of potassium phosphate buffer (0.1 M, pH 7.0).

SOD activity was determined based on its ability to inhibit nitroblue tetrazolium (NBT) photoreduction, following the method outlined by Dhindsa et al. (29). The activity of CAT was measured by the decrease in absorbance of the reaction mixture at 240 nm due to the decomposition of H₂O₂ (30). APx activity was assessed by monitoring the decrease in absorbance at 290 nm according to the method described by Nakano and Asada (31). The GPx assay involved measuring the absorbance of a light pink-coloured solution at 412 nm resulting from the colorimetric reaction between reduced glutathione and the 5,5'-dithiol-bis (2-nitrobenzoic acid) reagent (30). Under the standard assay conditions, one enzyme unit was defined as the amount of SOD required to inhibit NBT reduction by 50%, the quantity of CAT required to decompose 1.0 µM of H₂O₂, the amount of APx needed to convert 1 µM of H₂O₂ into H₂O, or the amount of GPx needed to generate 1.0 M of oxidized glutathione per min.

Statistical analysis

An entirely random design was employed. In the graphs, standard error (SE) values were utilized to depict data variability, and the results were presented as the mean of five separate replicates for all groups. The data analysis was conducted using one-way analysis of variance (ANOVA) and Tukey's test using IBM 26 SPSS software. The data was analyzed at a 5 % level of significance.

Results and Discussion

Characterization of NPs

As per the TEM images, CS NPs exhibited a size range of 4-8.5 nm (Fig. 1A), while TiO₂ NPs fell within the 35-76 nm range (Fig. 1B). The size spectrum for CS/TiO₂ NCPs spanned 60-80 nm (Fig. 1C). The surface morphology, as

revealed by FESEM images, showed that CS NPs had a rough, layered, and aggregated structure, resembling the notched surface of sedimentary rock (Fig. 1D). In contrast, TiO₂ NPs assumed a polygonal shape (Fig. 1E), whereas CS/TiO₂ NCPs manifested a novel structure resembling a coral-reef made up of whorls of petal-like structures with vast voids in between the whorls (Fig. 1F).

The hydrodynamic diameter and zeta potential of CS NPs, TiO₂ NPs and CS/TiO₂ NCPs as determined by the zeta sizer, were found to be 437.7, 369.1, and 2030 nm, and 11.4, 38.2, and -4.95, respectively (Fig. 2 A-F). In the NCPs, the interaction between TiO₂ NPs and CS likely exposed negative charges on the surface of CS/TiO₂ NCPs, resulting in their negative zeta potential. Based on the zeta potential values, it was concluded that both CS NPs and CS/TiO₂ NCPs were unstable. This instability could be attributed to the presence of various functional groups, such as -NH₂ and -OH, on their surface, which impart charges to the nanoparticles. The instability of these nanomaterials is closely linked to their ability to aggregate and react with other active substances to attain a relatively more stable state. Consistent with these findings, aggregation of CS NPs and CS/TiO₂ NCPs was also observed in their FESEM images (Fig. 1D and 1F, respectively).

The XRD technique was utilized to analyze the crystallographic structure of the synthesized NPs and NCPs as shown in Fig. 3 A, B and C. CS NPs exhibited a range of intense peaks at 18.66, 22.75, 32.19, 38.16, and 46.51 2theta diffraction angles, corresponding to 001, 100, 110, 111, and 200 hkl values, respectively (Fig. 3A) (32). For TiO₂ NPs, peaks were observed at 25.26, 37.86, 47.53, 54.30, and 62.28 2theta diffraction angles, with hkl values of 101, 004, 200, 105, and 204, consistent with JCPDS Card No. 21-1272 (Fig. 3B). The XRD analysis of CS/TiO₂ NCPs revealed peaks at 20.14, 25.32, 29.61, 38.03, 47.99, 54.30, 62.81, and 69.41 2theta values, with hkl values of 001, 101, 110, 004, 200, 211, 002 and 116, respectively (Fig. 3C). These findings were in good agreement with the previously reported peaks for these NCPs (15). The presence of various intense peaks in the XRD graphs of all nanomaterials indicates their crystalline nature, and no impurities were reported. The hkl values were calculated using equation (ii) and matched with those found in previous literature and their respective JCPDS cards.

$$\frac{1}{d^2} = \frac{h^2 + k^2 + l^2}{a^2} - \frac{c^2}{c^2} \dots \dots \dots \text{(ii)}$$

The average crystalline size of all the nanomaterials was calculated using Scherrer's equation and was found to be 6.90, 9, and 71 nm for CS NPs, TiO₂ NPs, and CS/TiO₂ NCPs, respectively.

The FTIR spectra for the CS and TiO₂ NPs and the CS/TiO₂ NCPs are presented in Fig. 3(D-F). In the FTIR spectra of CS NPs (Fig. 3D), the peaks at 3436 and 3285 cm⁻¹ were attributed to stretching vibrations of -OH and -NH₂, respectively, while the peak at 2923 cm⁻¹ was associated with -CH group stretching. The distinctive peak observed at 1648 cm⁻¹ was assigned to the presence of the CONH₂

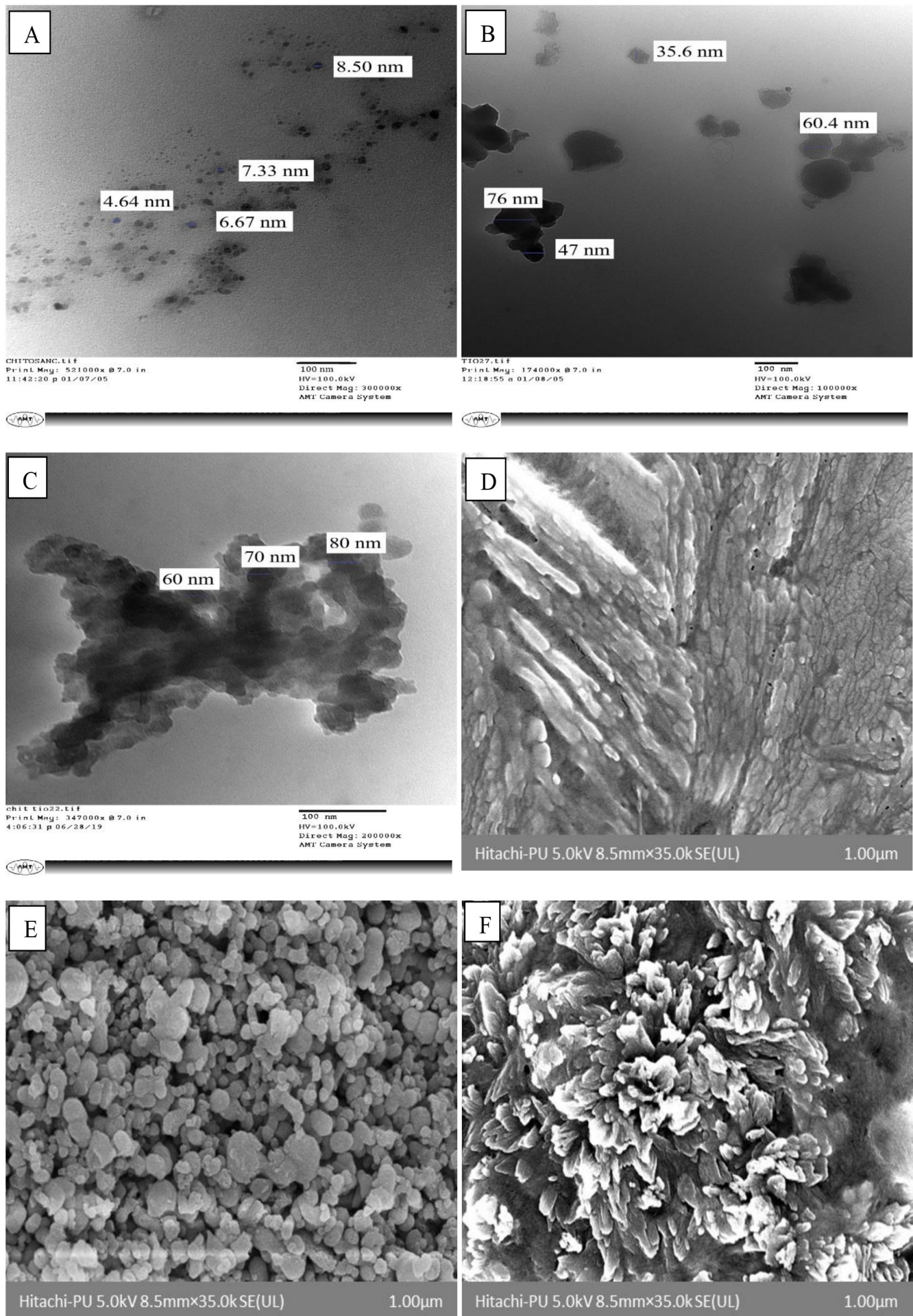


Fig. 1. TEM and FESEM images of CS NPs (A & D), TiO₂ NPs (B & E), and CS/TiO₂ NCPs (C & F), respectively

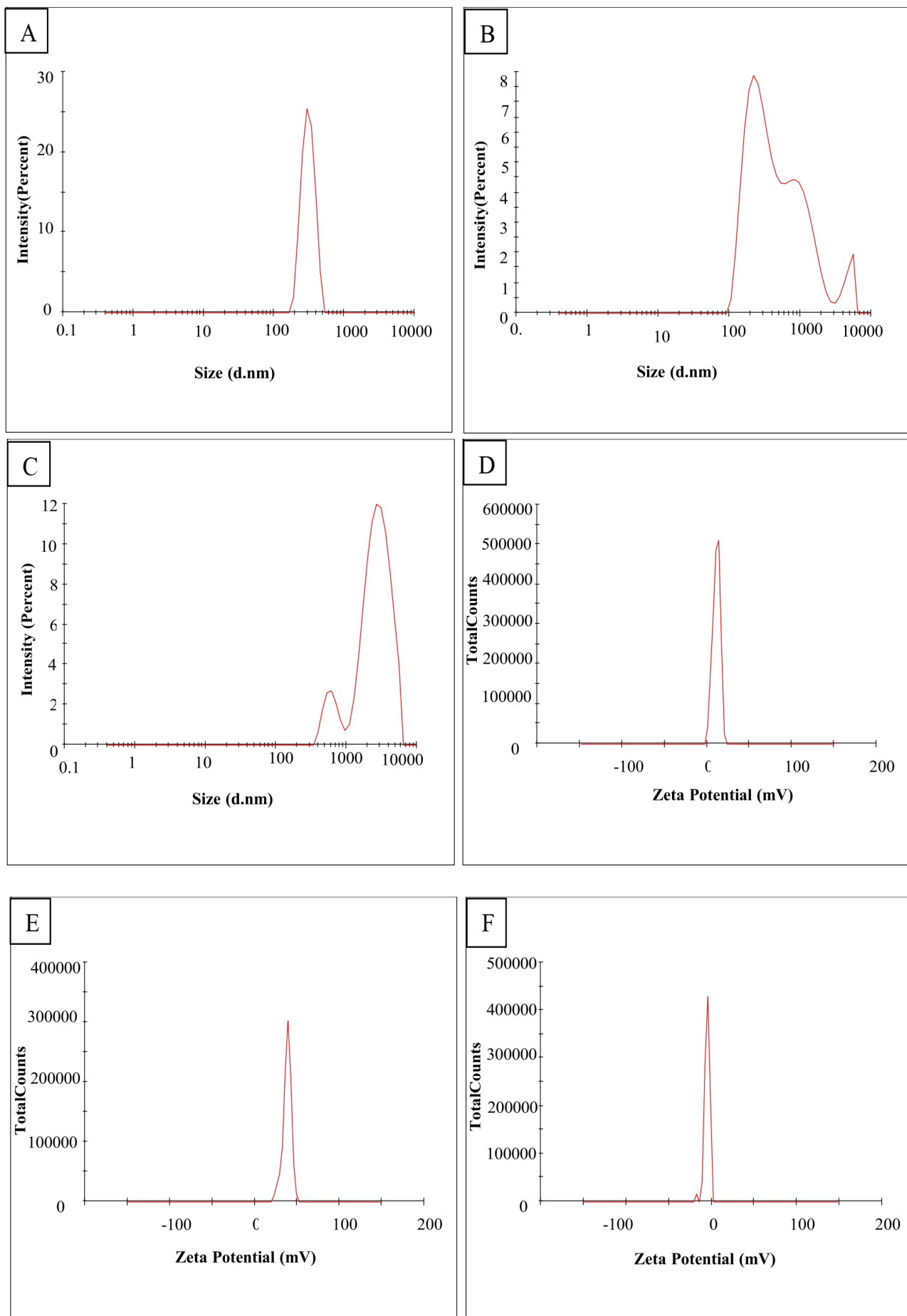


Fig. 2. Zeta sizer and Zeta potential graphs of CS NPs (A & D), TiO₂ NPs (B & E), and CS/TiO₂ NCPs (C & F), respectively

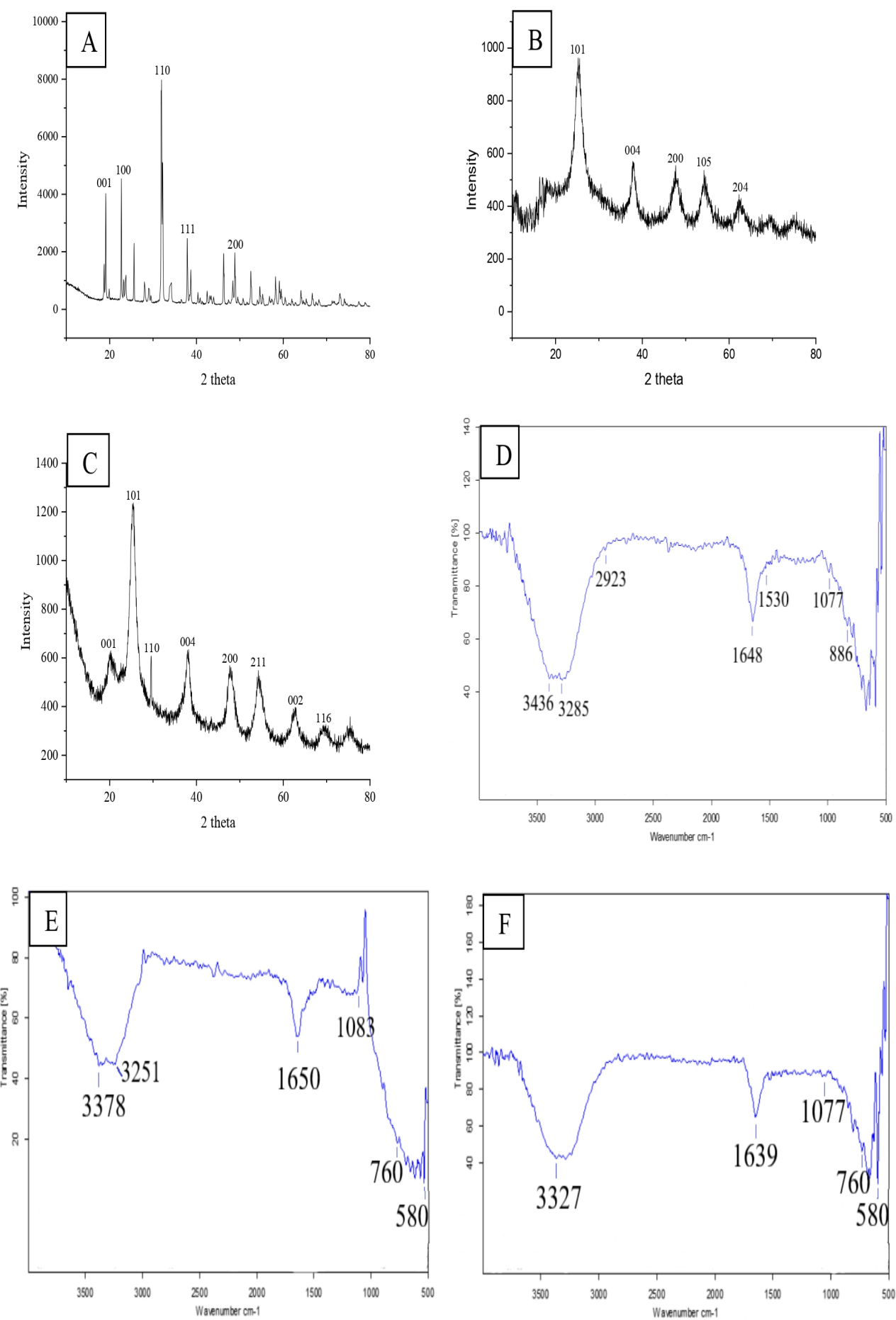


Fig. 3. XRD and FTIR analysis of CS NPs (A & D), TiO₂ NPs (B & E), and CS/TiO₂ NCPs (C & F), respectively

(amide) group. Additionally, the peaks at 1530cm^{-1} for -NH deformation, 1077 cm^{-1} for C-O-C stretching, and 886 cm^{-1} for glucopyranose ring of the CS matrix were identified (33). The peaks around 500 cm^{-1} correspond to out of plane bending of -NH and C-O groups in CS (34). In the FTIR spectra of TiO_2 NPs (Fig. 3E), the peaks at 3378 and 3251 cm^{-1} were due to the stretching of the -OH group, the peak at 1650 cm^{-1} was attributed to bending modes of aqueous Ti-OH , and the peaks at 1083 and between $700\text{-}500\text{ cm}^{-1}$ were indicative of Ti-O bond stretching, confirming the formation of TiO_2 NPs (35). In the FTIR spectrum of the CS and TiO_2 NCPs (Fig. 3F), peaks corresponding to both CS and TiO_2 NPs were observed, and the peaks associated with CS showed a slight shift due to the formation of NCPs. The peaks at 3327 , 1639 , and 1077 cm^{-1} were linked to stretching of the -OH groups, an amide bond, and C-O-C stretching, respectively, indicative of the CS component. The stretching vibrations of the Ti-O bond in TiO_2 were observed at 760 and 580 cm^{-1} .

Soil analysis

S. bicolor plants were grown in pots filled with soil having a pH of 7.02 , an electrical conductivity of 0.29 dS m^{-1} , and an organic carbon content of 0.66% . The macronutrient profile of the soil showed concentrations of 20 ppm N , 11 ppm P , 54 ppm K , and $13.23\text{ ppm sulphur (S)}$. Additionally, the micronutrient analysis revealed the presence of $2.73\text{ ppm zinc (Zn)}$, $19.62\text{ ppm iron (Fe)}$, $4.20\text{ ppm manganese (Mn)}$, and $1.04\text{ ppm copper (Cu)}$. For optimal plant growth, the soil pH should range from 6.5 to 8.5 , the electrical conductivity should be below 0.8 dS m^{-1} , and the organic carbon content should be less than 0.4% . Essential soil micronutrients should maintain minimum levels of 0.6 ppm of Zn , 4.5 ppm for Fe , 2 ppm for Mn , 0.2 ppm for Cu , and $10\text{ ppm for }S. bicolor$ thrives in soils with a pH between 6 and 7.5 , a range that enables plant roots to absorb nutrients more efficiently. The electrical conductivity, organic carbon, and nutrient levels of the soil were within the ideal range for *S. bicolor* cultivation. The organic matter in the soil plays a crucial role in keeping NPs dispersed, preventing their agglomeration, and facilitating easy uptake by plants (36).

Effect on growth parameters

The growth of 30-day-old *S. bicolor* plants was observed to be stimulated at both concentrations (100 and 200 ppm) of CS NPs, TiO_2 NPs, and their NCPs compared to controls (Table 1). Among CS NPs, TiO_2 NPs, and CS/ TiO_2 NCPs, the maximum stimulation in shoot and root growth of *S. bicolor* was observed with TiO_2 NPs. CS NPs increased the length, freshness, and dry weight of shoots by approximately 10% at 100 ppm , while the increase slightly dropped at 6% , 7% , and 5% , respectively, at 200 ppm . Similarly, the length and fresh weight of the roots increased by 8% at 100 ppm , and by only 3% at 200 ppm . At 200 ppm of CS NPs, root dry weight was comparable to control plants, whereas at 100 ppm , it increased slightly by 6% . Previous studies have also reported the stimulatory effects of CS on plant growth. Sathyabama and Manikandan (5) found that foliar application of 0.1% CS enhanced the growth of finger millet plants. Divya et al. (37) reported an increase in growth of rice plants by 1 mg mL^{-1} CS NPs, suggesting that the enhancement in the plant growth was due to CS NPs-induced enhancement in nutrient uptake.

TiO_2 NPs stimulated both shoot and root growth at concentrations of 100 and 200 ppm . The shoot length, fresh weight, and dry weight increased by approximately 23% at 100 ppm and 15% at 200 ppm , respectively. Additionally, TiO_2 NPs increased root length and root fresh weight by 22% compared to the control plants, and root dry weight by 19% at 100 ppm . At 200 ppm , the percent enhancement in root length, fresh weight and dry weight was approximately 13% . Thakur et al. (25) also reported increased biomass, root, and shoot length in mung bean plants grown in a hydroponic setup with two different concentrations of TiO_2 NPs (10 and 100 mg L^{-1}). The hydroxy radicals produced by TiO_2 NPs cause the cell wall to loosen, leading to cell enlargement and growth (25).

CS/ TiO_2 NCPs also demonstrated a positive impact on shoot and root growth. The shoot length, shoot freshness, and dry weight were increased by approximately 15% at 100 ppm and by 16% at 200 ppm . At

Table 1. Effect of CS NPs, TiO_2 NPs and CS/ TiO_2 NCPs on the growth of 30-days-old *S. bicolor* plants

S. No.	Treatments (ppm)	Shoot length (cm)	Shoot fresh weight (g)	Shoot dry weight (g)	Root length (cm)	Root fresh weight (g)	Root dry weight (g)	
2.	Control (0)	73.3 ± 3.24^b	6.66 ± 0.09^d	0.80 ± 0.02^b	32.26 ± 2.52^a	0.90 ± 0.03^b	0.16 ± 0.04^a	
	100	80.88 ± 3.52^{ab}	7.35 ± 0.12^{bc}	0.88 ± 0.04^{ab}	34.94 ± 2.56^a	0.97 ± 0.03^b	0.17 ± 0.04^a	
	200	77.42 ± 1.92^{ab}	7.13 ± 0.16^{cd}	0.84 ± 0.05^{ab}	33.14 ± 2.61^a	0.93 ± 0.02^b	0.16 ± 0.004^a	
3.	TiO_2 NPs	100	90.14 ± 3.27^a	8.17 ± 0.08^a	0.98 ± 0.02^a	39.32 ± 1.00^a	1.10 ± 0.02^a	0.19 ± 0.02^a
		200	84.2 ± 0.44^{ab}	7.65 ± 0.09^{abc}	0.92 ± 0.02^{ab}	36.3 ± 1.97^a	1.02 ± 0.03^{ab}	0.18 ± 0.04^a
	CS/ TiO_2 NCPs	100	84.52 ± 2.43^{ab}	7.68 ± 0.1^{abc}	0.92 ± 0.02^{ab}	33.18 ± 1.14^a	0.93 ± 0.02^b	0.16 ± 0.004^a
4.	CS/ TiO_2 NCPs	200	85.46 ± 3.86^{ab}	7.76 ± 0.25^{ab}	0.93 ± 0.04^{ab}	35.44 ± 1.63^a	0.98 ± 0.03^b	0.17 ± 0.004^a

Data is presented as mean \pm S.E. ($n = 5$) and different letters indicate the significant difference at $p < 0.05$

a concentration of 100 ppm, the enhancement in root length and root fresh weight was 3%, while there was no significant difference in root dry weight compared to the control plants. At 200 ppm, there was an approximately 10% increase in root length, a 9% increase in root fresh weight, and a 6% increase in root dry weight.

Effect of NPs on uptake of nutrients

CS NPs, TiO₂ NPs and CS/TiO₂ NCPs were found to enhance the uptake of nutrients from the soil (Table 2). The N and K content was highest in the shoot and roots of TiO₂NPs treated plants, followed by those treated with CS/TiO₂ NCPs and CS NPs treated plants. Conversely, Mg and P levels were highest in the shoot and roots of plants treated with CS/TiO₂ NCPs, followed by TiO₂ NPs and CS NPs treated plants. Nevertheless, all treatment groups exhibited significantly higher nutrient accumulation compared to control plants. These findings were consistent with previous literature.

The larger surface area of NPs, which can retain nutrients on their surface and increase their bioavailability, likely contributes to enhanced nutrient absorption in the presence of NPs (38). A study by O'Herlihy et al. (39) demonstrated that potato plants significantly increased their uptake of plant nutrients following the application of CS solution. Similarly, the addition of 1% CS to fertilizer boosted the N and P content of *Eustoma grandiflorum* (Raf) plants compared to those grown in soil without CS (40). CS contains numerous amino groups, including N, suggesting it may serve as a source of N for plants (41). Furthermore, CS has demonstrated a positive impact on the growth of rhizobacteria, as it forms a symbiotic relationship with rhizobacteria that promotes plant nutrient uptake (42). Additionally, studies have found that TiO₂ NPs can improve the uptake of nitrates, leading to increased N content in treated spinach plants (10).

Table 2. Uptake of nutrients in control and treated *S. bicolor* plants after 30 days of growth

Treatments (ppm)/ Nutrients (%)	Control (0)	CS NPs		TiO ₂ NPs		CS/TiO ₂ NCPs	
		100	200	100	200	100	200
N Shoot	1.60±0.012 ^f	2.14±0.017 ^e	2.09±0.004 ^e	3.01±0.026 ^a	2.26±0.017 ^d	2.53±0.004 ^c	2.83±0.013 ^b
N Root	2.81±0.006 ^e	2.93±0.008 ^c	2.84±0.004 ^d	3.98±0.007 ^a	3.3±0.006 ^b	2.94±0.005 ^c	2.84±0.007 ^d
K Shoot	2.94±0.016 ^f	3.86±0.007 ^d	3.80±0.012 ^{de}	5.45±0.011 ^a	4.42±0.004 ^c	4.90±0.026 ^b	3.79±0.009 ^e
K Root	2.13±0.004 ^g	4.31±0.02 ^c	3.08±0.007 ^f	4.84±0.006 ^a	3.18±0.007 ^e	4.11±0.005 ^d	4.47±0.004 ^b
Mg Shoot	0.34±0.003 ^f	0.45±0.005 ^{de}	0.42±0.005 ^e	0.53±0.005 ^b	0.49±0.005 ^c	0.59±0.012 ^a	0.46±0.01 ^{cd}
Mg Root	0.24±0.007 ^d	0.45±0.006 ^b	0.55±0.009 ^a	0.53±0.003 ^a	0.35±0.009 ^c	0.44±0.009 ^b	0.24±0.005 ^d
P Shoot	0.22±0.003 ^{cd}	0.23±0.004 ^c	0.20±0.006 ^{de}	0.23±0.004 ^c	0.18±0.004 ^e	0.31±0.004 ^b	0.37±0.007 ^a
P Root	0.20±0.003 ^f	0.29±0.004 ^e	0.28±0.01 ^e	0.40±0.005 ^c	0.35±0.003 ^d	0.75±0.009 ^a	0.56±0.005 ^b

Data is presented as mean ± S.E. (n = 5) and different letters indicate the significant difference at p<0.05

Total chlorophyll content

One of the most crucial elements needed to sustain photosynthetic capacity is the content of chlorophyll. Chlorophyll levels significantly increased in all the treated plants, indicating that the presence of CS and TiO₂ NPs, and CS/TiO₂ NCPs improved the general health and photosynthetic capacity of plants (Fig. 4A). The highest chlorophyll content was found in CS/TiO₂ NCPs treated *S. bicolor* plants, where the amount of chlorophyll almost doubled with an increment of 93% at 100 ppm and 94% at 200 ppm concentration. Chlorophyll content in TiO₂ NPs treated plants increased by 75% at 100 ppm and 62% at 200 ppm. The least increase in chlorophyll was observed for CS NPs treated plants, where chlorophyll contents increased by 57% and 35% at 100 and 200 ppm, respectively. Compared to the control group, an increase in the chlorophyll content of all the treated plants correlates well with the increased uptake of N and Mg by these plants.

Van et al. (43) found that foliar spraying of CS NPs (30-50%) increased chlorophyll content in coffee plants. Similarly, both soil and foliar application of CS NPs enhanced the chlorophyll content of *Triticum aestivum* L. (41), and *Catharanthus roseus* (L.) G. Don (44), when grown under drought conditions. CS NPs may enhance the availability of free amino compounds and the internal cytokinin levels, thereby triggering the production of chlorophyll synthesis genes and increasing chlorophyll levels (45). Furthermore, the antioxidant activity of CS inhibits the degradation of photosynthetic pigments and scavenges reactive oxygen species (ROS) in thylakoids. Additionally, these NPs may improve photosynthetic efficiency by boosting the activity of Rubisco carboxylase and by inhibiting ethylene, which stimulates chlorophyllase (46).

Song et al. (21) reported increased chlorophyll content in *Lemna minor* L. plants at various concentrations of TiO₂ NPs, from 10, 50, 100, 200, 500, 1000 and 2000 mg L⁻¹. TiO₂ NPs were also found to stimulate chlorophyll contents in *Mentha piperita* L. (47). Although the specific mechanism for TiO₂ NPs induced rise in chlorophyll content is uncertain, it has been suggested that it may occur due to enhanced Fe uptake (25), which is needed for the conversion of protoporphyrin to a chlorophyll precursor. The inclusion of both CS and TiO₂ NPs in the NCPs may have synergistic effects, leading to a substantial increase in the chlorophyll content of plants treated with CS/TiO₂ NCPs.

Starch and cellulose content

Compared to control plants, the starch content in the shoots of 30-days-old *S. bicolor* plants was increased by CS NPs, TiO₂ NPs, and their NCPs at both concentrations. However, a significant increase was observed only for the plants treated with CS/TiO₂ NCPs (Fig. 4B). The CS/TiO₂ NCPs increased the starch content in the shoots of *S. bicolor* by 19% at both 100 and 200 ppm concentrations. Through photosynthesis, chlorophyll produces energy in the form of carbohydrates, storing the surplus as starch (21). The increase in chlorophyll content might have increased the photosynthetic assimilation in these plants, resulting in better sugar and hence, starch production. In addition to chlorophyll content, starch content is also influenced by K uptake by plants. The shoots of all NP-treated plants showed higher K uptake, which might have led to increased starch synthesis as K is an activator of the starch synthase enzyme (48). Elevated starch levels in the stem and leaves of high biomass crops such as *S. bicolor* improve forage quality and the efficiency of biomass conversion to biofuels and bioproducts.

Since *S. bicolor* bagasse contains up to 31.42% cellulose, it emerges as a potential source of cellulose fibre. Typically used in the production of fibre-based products and other low-value applications such as combustion, hay for animal feed and bedding, biochemical production, and as a source of organic matter to enhance soil water retention, fertility, and to prevent soil erosion. *S. bicolor* offers versatile utility. In the present work, an increase in the cellulose content of *S. bicolor* shoots was observed for all the treatment groups compared to the control group (Fig. 4C). CS NPs increased the cellulose content by 20% at 100 ppm and by 26% at 200 ppm concentration. TiO₂ NPs resulted in a 13% and 18% increase in cellulose content at 100 and 200 ppm concentrations, respectively. In contrast, CS/TiO₂ NCPs significantly augmented the cellulose content at 36% and 56% at 100 and 200 ppm concentrations, respectively, in the shoots of *S. bicolor* plants. Cellulose is critical for maintaining the integrity of plant cell walls and supporting growth. Thus, the enhancement of cellulose content is consistent with the observed growth promotion of *S. bicolor* in the presence of NPs.

Protein content

CS/TiO₂ NCPs significantly increased the protein content in the shoots of 30-day-old *S. bicolor* plants (Fig. 4D). Protein content increased by 119% at 100 ppm and 78% at 200

ppm concentrations of NCPs. Similarly, TiO₂ NPs enhanced the protein content of the shoot, while the protein content in the shoot of CS NPs treated plants remained comparable to that of the control plants. Moreover, the protein content of the roots in all treated plants did not show a significant difference from that of the control plants. The increased protein content attributed to CS/TiO₂ NCPs and TiO₂ NPs may result from improved N uptake, which is crucial for synthesizing proteins and amino acids (45). Additionally, TiO₂ NPs facilitate the transformation of NH₄⁺-N into organic nitrogen (10). Similar results were reported by Dowom et al. (46), who observed no significant increase in protein content with CS NPs at concentrations of 30, 60, and 90 ppm in *Salvia abrotanoides* (Kar.) Sytsma. Furthermore, TiO₂ NPs increased the protein content of the spinach plant at a concentration of 0.25% and *Cicer arietinum* L. plants at 1000 ppm (3, 10).

Lipid peroxidation

Lipid peroxidation, indicative of cellular oxidative damage, can be assessed by measuring the MDA content in the cells. In our study, both CS NPs, and TiO₂ NPs, as well as CS/TiO₂ NCPs at concentrations of 100 and 200 ppm, demonstrated a reduction in MDA content in the shoots of *S. bicolor* plants (Fig. 4E). Conversely, there was an increase in the MDA content in the roots of the treated plants. Specifically, the shoots of 30-day-old *S. bicolor* plants exhibited a significant reduction in MDA content by 24% and 22% at concentrations of 100 and 200 ppm of CS NPs, respectively. Notably, the highest levels of MDA were detected in the roots of TiO₂ NPs treated plants, followed by those treated with CS/TiO₂ NCPs. At concentrations of 100 and 200 ppm of TiO₂ NPs and CS/TiO₂ NCPs, the percent increase in MDA content was 75 and 80 and 44 and 41, respectively.

The observed increase in MDA content in roots suggests that NPs primarily affect root cells. However, this did not inhibit root growth, possibly due to the efficient neutralization of ROS by the antioxidant machinery of the cell. This finding is consistent with previous research; for instance, Faizan et al. (24) reported that a foliar spray of CS NPs (100 µg mL⁻¹) reduced MDA content in tomato leaves. Conversely, Mohammadi et al. (49) reported an increase in MDA content induced by TiO₂ NPs in *Dracocephalum moldavica* L. roots at concentrations of 10 and 20 ppm. Additionally, while the MDA content of oakleaf lettuce plants did not initially increase with TiO₂ NPs at a concentration of 0.75%, it did so on the 7th day post application (50). In contrast, Latef et al. (12) found no discernible difference in MDA levels in broad bean plants treated with 0.01 to 0.03% TiO₂ NPs.

Antioxidant enzymes

Various types of ROS are generated in plant tissues through metabolic reactions, photosynthetic reactions, and periods of stress. To counteract the harmful effects of ROS, cells deploy antioxidant molecules, which play a crucial role in maintaining homeostasis within plant tissues. In the present study, the determination of antioxidant enzymes, including SOD, CAT, APx, and GPx,

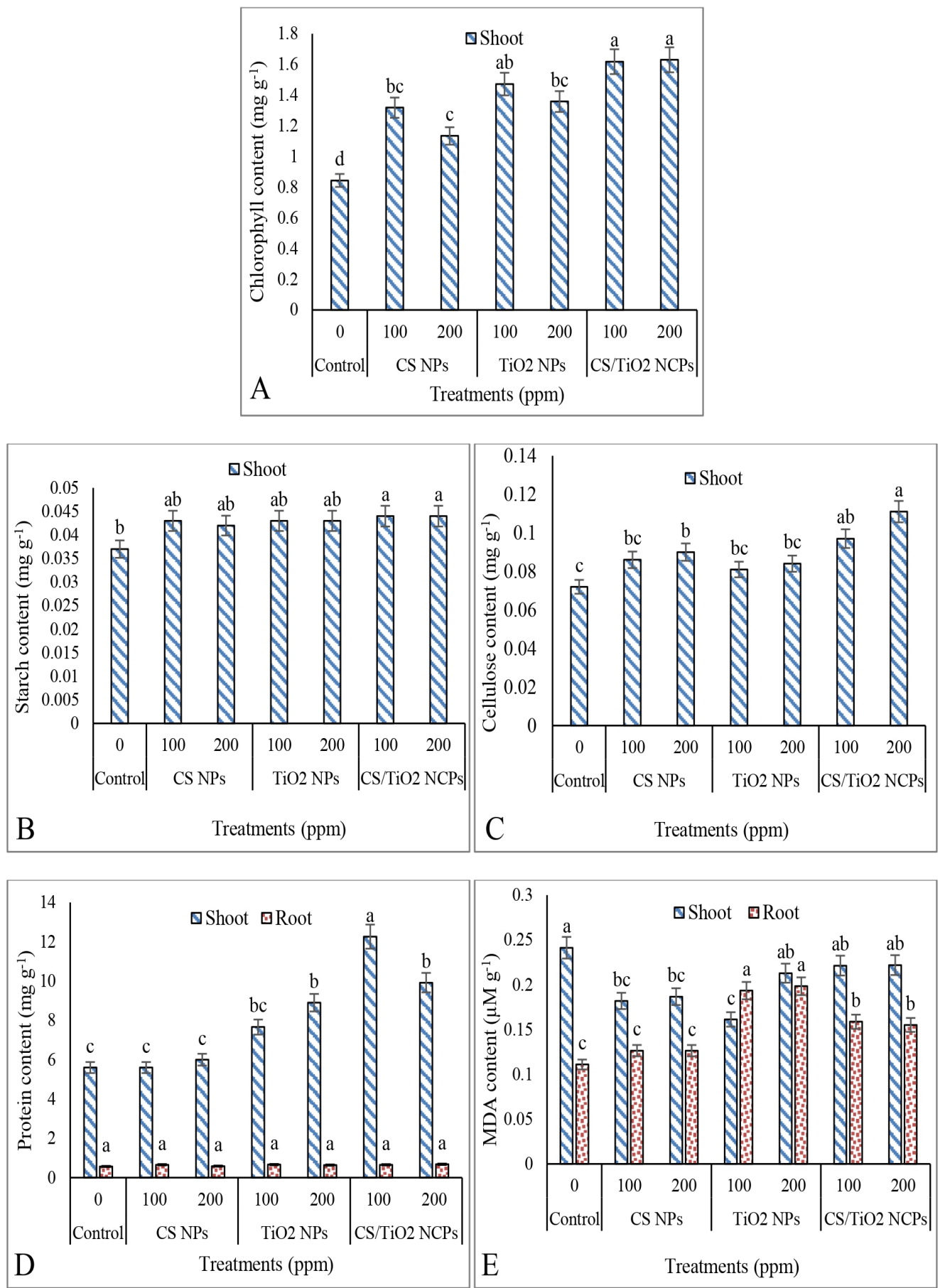


Fig. 4. Bar graph showing the effect of CS NPs, TiO₂ NPs, and CS/TiO₂ NCPs on chlorophyll (A), starch (B), cellulose (C), protein (D) and MDA (E) contents of 30-days-old *S. bicolor* plants. The results are presented as means of five different replicates, with the variability of data represented by standard error bars. Different letters indicate the significant differences at $p<0.05$.

provided valuable insights into the changes in the antioxidant status of the plants following treatment.

Slight fluctuations, including both increases and decreases, were observed in shoot SOD activity across all treatment groups, with no statistically significant differences compared to the control plant SOD activity in the shoot. However, a significant increase in root SOD activity was noted in TiO₂ NPs and CS/TiO₂ NCPs treated plants at both 100 and 200 ppm concentrations (Fig. 5A). The CAT activity was significantly higher in the shoots of TiO₂ NPs and CS/TiO₂ NCPs treated plants at both 100 and 200 ppm concentrations, while relatively little variation was observed in the CAT activity of the roots of the treated plants, comparable to the activity of CAT in control plant roots (Fig. 5B). Conversely, APx activity decreased significantly in both the roots and shoots of all the treated plants (Fig. 5C). GPx activity increased significantly in the shoots of CS/TiO₂ NCPs treated plants at both concentrations, while no significant differences were observed in GPx activity in other treated plants compared to control plants (Fig. 5D).

Alteration in the activity of antioxidant enzymes is a natural mechanism adopted by plants to maintain H₂O₂ homeostasis. Within the cell, SOD converts singlet oxygen and superoxide radicals to H₂O₂, while CAT and GPx work together to neutralize and eliminate H₂O₂. SOD serves as the primary defense enzyme against harmful radicals, eliminating superoxide and minimizing damage to metabolic processes. Although the shoots of CS and TiO₂ NPs, and CS/TiO₂ NCPs treated *S. bicolor* plants exhibited reduced ROS production, as indicated by decreased MDA contents, an increase in shoot CAT by TiO₂ NPs and in shoot CAT and GPx by CS/TiO₂ NCPs suggests increased H₂O₂ production in these plants. Similarly, the high MDA content and hence high ROS concentration in the roots of TiO₂ NPs and CS/TiO₂ NCPs treated plants, along with the increased activity of root SOD, indicate a compensatory antioxidant defense mechanism adopted by plants. ROS production is often exacerbated in actively photosynthesizing plants due to the photolysis of water.

Indeed, additional factors contribute to the overproduction of ROS in plants. These include the

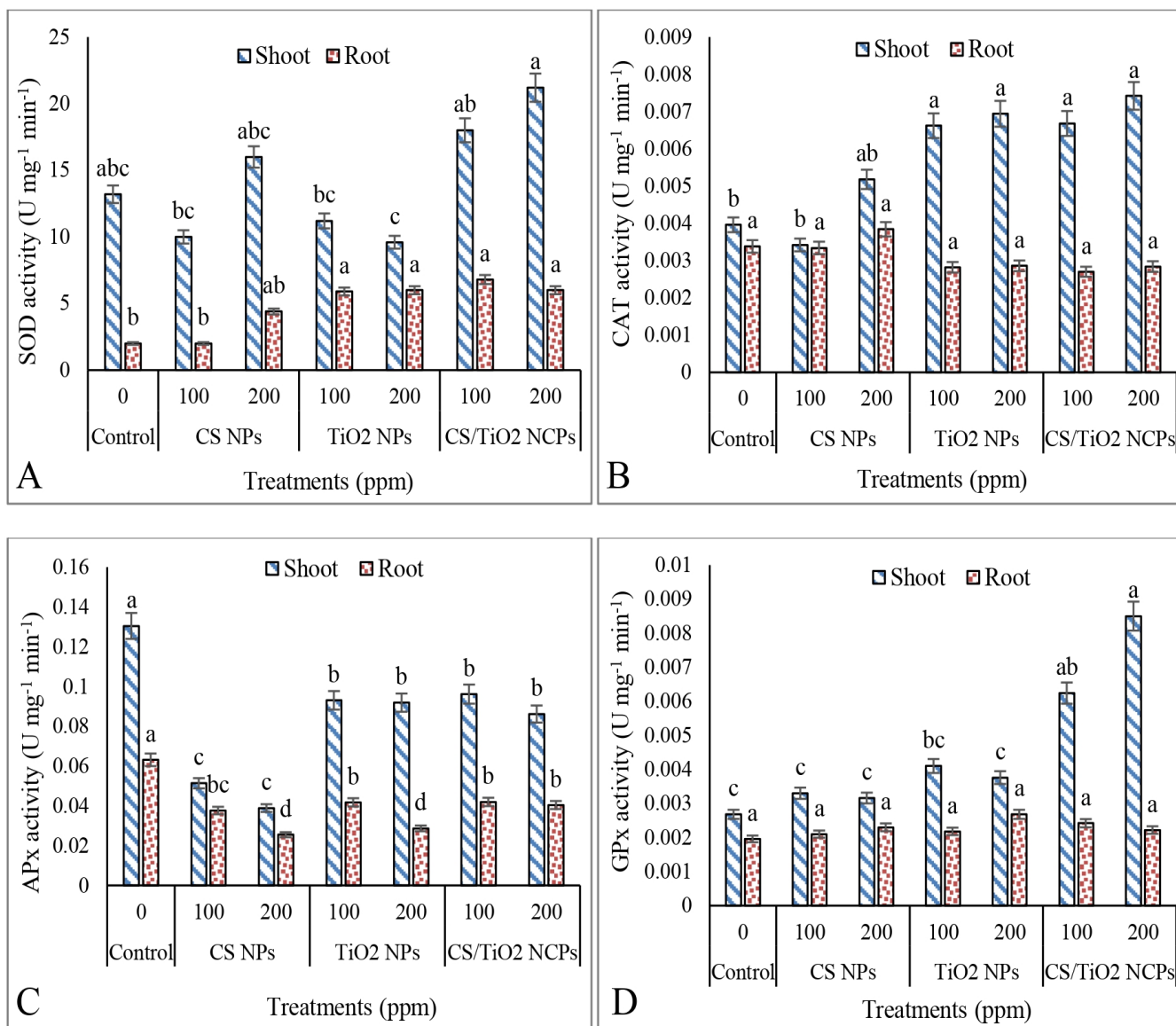


Fig. 5. Bar graph showing the effect of CS NPs, TiO₂ NPs, and CS/TiO₂ NCPs on the activities of antioxidant enzymes of 30-days-old *S. bicolor* plants: SOD (A), CAT (B), APx (C) and GPx (D). The values are means of five replicates, variability of data is represented by standard error bars. Different letters indicate the significant differences at $p < 0.05$.

transport of electrons through Fe-S centres, the ferredoxin/ thioredoxin redox system, stimulation of NADPH oxidase, and other biological redox reactions. These processes often lead to increased ROS levels, which are typically counteracted by upregulating the activities of antioxidant enzymes. Moreover, interactions between thylakoid membrane pigments and oxygen can generate strong oxidants. The higher chlorophyll levels observed in TiO₂ NPs and CS/TiO₂ NCPs treated plants may have directly increased ROS production, thereby augmenting the activities of SOD in roots and CAT and GPx in the shoots of these plants. According to several studies, nanomaterials have been shown to increase antioxidant enzyme activities, thereby reducing ROS accumulation and enhancing growth and photosynthesis. SOD, CAT, and GPx work together to neutralize singlet oxygen and H₂O₂, preventing the generation of more harmful radicals and stabilizing cellular activity. The findings of this study are consistent with those of Hassan et al. (13), who demonstrated that the foliar application of saffron dye-coated TiO₂ NPs at 500 ppm enhanced the activity of antioxidant enzymes, including CAT, in *S. bicolor*. TiO₂ NPs have also been found to increase SOD and CAT activities in *L. minor* L. (21) and mung bean (25). Similarly, CS NPs did not significantly increase the SOD activities in *S. abrotanoides* (Kar.) Sytsma (46).

Conclusion

In conclusion, the positive impact of CS NPs, TiO₂NPs, and their respective NCPs on the growth of *S. bicolor* is attributed to enhanced uptake of vital nutrients, including N, K, Mg, and P. This improved nutritional status, along

with increased chlorophyll levels, resulted in elevated starch and cellulose content in the treated plants compared to the control group. It is noteworthy that mild oxidative stress was observed in the roots of TiO₂ NPs (200 ppm) and CS/TiO₂ (100 and 200 ppm) NCPs treated plants, which was effectively managed by the antioxidant machinery of the treated plants. These findings provide valuable insights for future research endeavours exploring the application of nanomaterials in agriculture.

Acknowledgements

The authors acknowledge the financial support from DST, New Delhi (FIST grant no. SR/FST/LS1-529/2012(C)) and HSCSIT, Panchkula, Haryana (Endst. No. HSCSIT/R&D/2020/474).

Authors' contributions

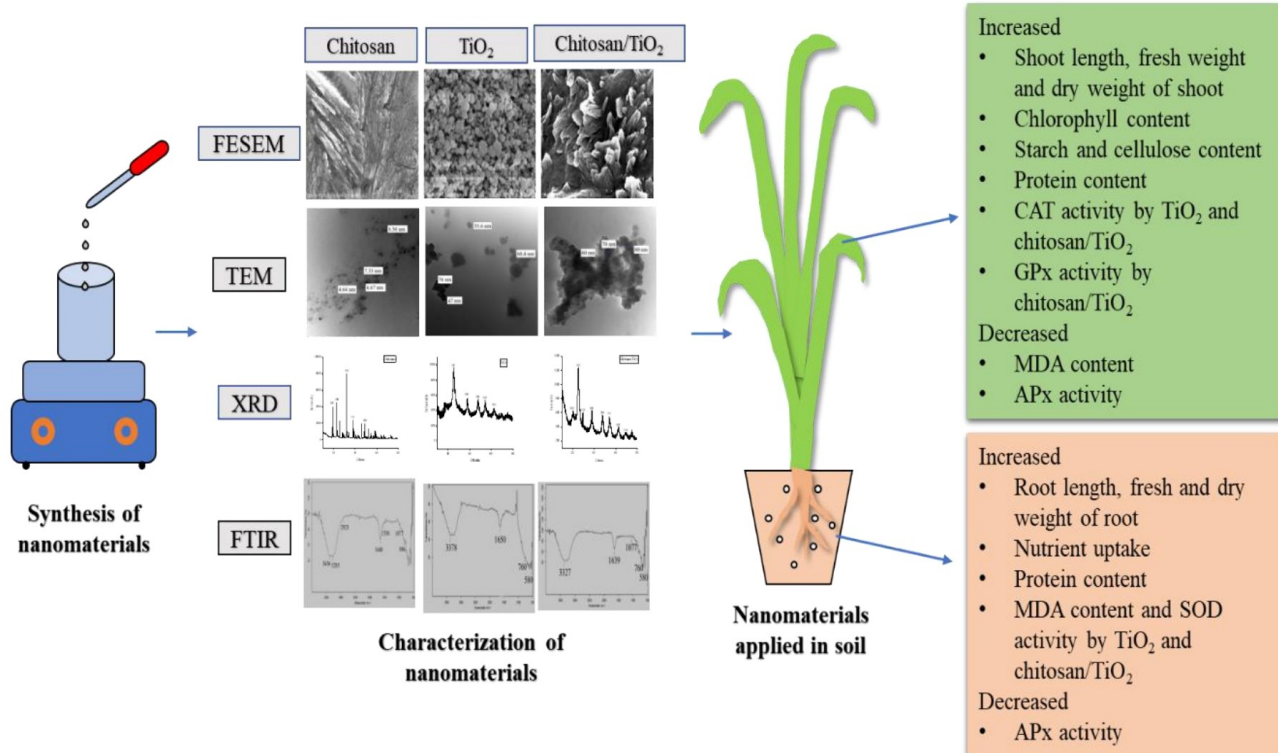
VH conceived the idea and finalized the study design. NR conducted background study, experiments, and collected the data. NR and KK carried out the data analysis. KK assisted in graphical representation of the data. NR wrote the original manuscript draft, while VH reviewed, edited, corrected and finalized it. All the authors approved the manuscript in its present form.

Compliance with ethical standards

Conflict of interest: Authors do not have any conflict of interests to declare.

Ethical issues: None.

Graphical abstract



References

1. Ditta A. How helpful is nanotechnology in agriculture? Advances in Natural Sciences: Nanoscience and Nanotechnology. 2012;3:033002. <https://doi.org/10.1088/2043-6262/3/3/033002>
2. Abdel-Rahman Ismael S. Physiological and biochemical responses of Jew's mallow (*Cochrinos olitorius* L.) to foliar spray of nanosized ZnO. Plant Science Today. 2023;10:312-20. <https://doi.org/10.14719/pst.2311>
3. Hajra A, Mondal NK. Effects of ZnO and TiO₂ nanoparticles on germination, biochemical and morphoanatomical attributes of *Cicer arietinum* L. Energy, Ecology and Environment. 2017;2:277-88. <https://doi.org/10.1007/s40974-017-0059-6>
4. Li R, He J, Xie H, Wang W, Bose SK, Sun Y et al. Effects of chitosan nanoparticles on seed germination and seedling growth of wheat (*Triticum aestivum* L.). International Journal of Biological Macromolecules. 2019;126:91-100. <https://doi.org/10.1016/j.ijbiomac.2018.12.118>
5. Sathiyabama M, Manikandan A. Foliar application of chitosan nanoparticle improves yield, mineral content and boosts innate immunity in finger millet plants. Carbohydrate Polymers. 2021;258:117691. <https://doi.org/10.1016/j.carbpol.2021.117691>
6. Agricultural Market Intelligence Centre, ANGRAU, Lam. Sorghum Outlook Report-January to May 2021.
7. Srivastava A, Kumar SN, Aggarwal PK. Assessment on vulnerability of sorghum to climate change in India. Agriculture, Ecosystems and Environment. 2010;138:160-69. <https://doi.org/10.1016/j.agee.2010.04.012>
8. Maity A, Natarajan N, Pastor M, Vijay D, Gupta CK, Wasnik VK. Nanoparticles influence seed germination traits and seed pathogen infection rate in forage sorghum (*Sorghum bicolor*) and Cowpea (*Vigna unguiculata*). Indian Journal of Experimental Biology. 2018;56:363-72.
9. Djanaguiraman M, Nair R, Giraldo JP, Prasad PVV. Cerium oxide nanoparticles decrease drought-induced oxidative damage in sorghum leading to higher photosynthesis and grain yield. ACS Omega. 2018;3:14406-16. <https://doi.org/10.1021/acsomega.8b01894>
10. Yang F, Hong F, You W, Liu C, Gao F, Wu C, Yang P. Influence of nano-anatase TiO₂ on the nitrogen metabolism of growing spinach. Biological Trace Element Research. 2006;110:179-90. <https://doi.org/10.1385/BTER:110:2:179>
11. Lei Z, Mingyu S, Xiao W, Chao L, Chunxiang Q, Liang C et al. Antioxidant stress is promoted by nano-anatase in spinach chloroplasts under UV-B radiation. Biological Trace Element Research. 2008;121:69-79. <https://doi.org/10.1007/s12011-007-8028-0>
12. Latef AAHA, Srivastava AK, El-sadek MSA, Kordrostami M, Tran LSP. Titanium dioxide nanoparticles improve growth and enhance tolerance of broad bean plants under saline soil conditions. Land Degradation and Development. 2018;29:1065-73. <https://doi.org/10.1002/lrr.2780>
13. Hassan M, Ahangar AG, Mir N. Effect of TiO₂ nanoparticles with high light absorption on improving growth parameters and enzymatic properties of sorghum (*Sorghum bicolor* L. Moench). Journal of Nano Research. 2022;75:29-40. <https://doi.org/10.4028/p-dorek7>
14. Moll J, Klingensfuss F, Widmer F, Gogos A, Bucheli TD, Hartmann M, van der Heijden MG. Effects of titanium dioxide nanoparticles on soil microbial communities and wheat biomass. Soil Biology and Biochemistry. 2017;111:85-93. <https://doi.org/10.1016/j.soilbio.2017.03.019>
15. Karthikeyan KT, Nithya A, Jothivenkatachalam K. Photocatalytic and antimicrobial activities of chitosan-TiO₂ nanocomposite. International Journal of Biological Macromolecules. 2017;104:1762-73. <https://doi.org/10.1016/j.ijbiomac.2017.03.121>
16. Haldorai Y, Shim J. Novel chitosan-TiO₂ nanohybrid: Preparation, characterization, antibacterial and photocatalytic properties. Polymers Composites. 2014;35:327-33. <https://doi.org/10.1002/pc.22665>
17. Mesgari M, Aalami AH, Sahebkar A. Antimicrobial activities of chitosan/titanium dioxide composites as a biological nanolayer for food preservation: A review. International Journal of Biological Macromolecules. 2021;176:530-39. <https://doi.org/10.1016/j.ijbiomac.2021.02.099>
18. Al-Nemrawi N, Nimrawi S. A novel formulation of chitosan nanoparticles functionalized with titanium dioxide nanoparticles. Journal of Advanced Pharmaceutical Technology and Research. 2021;12:402-07. [10.4103/japtr.japtr_22_21](https://doi.org/10.4103/japtr.japtr_22_21)
19. Govindan S, Nivethaa EAK, Saravanan R, Narayanan V, Stephen A. Synthesis and characterization of chitosan-silver nanocomposite. Applied Nanoscience. 2012;2:299-303. <https://doi.org/10.1007/s13204-012-0109-5>
20. Ghows N, Entezari MH. Ultrasound with low intensity assisted the synthesis of nanocrystalline TiO₂ without calcination. Ultrasonics Sonochemistry. 2010;17:878-83. <https://doi.org/10.1016/j.ultsonch.2010.03.010>
21. Song G, Gao Y, Wu H, Hou W, Zhang C, Ma H. Physiological effect of anatase TiO₂ nanoparticles on *Lemna minor*. Environmental Toxicology and Chemistry. 2012;31:2147-52. <https://doi.org/10.1002/etc.1933>
22. Haghghi M, Silva JAT. The effect of N-TiO₂ on tomato, onion and radish seed germination. Journal of Crop Science and Biotechnology. 2014;17:221-27. <https://doi.org/10.1007/s12892-014-0056-7>
23. Behboudi F, Sarvestani TZ, Kassaei MZ, Sanavi SAMM, Sorooshzadeh A. Phytotoxicity of chitosan and SiO₂ nanoparticles to seed germination of wheat (*Triticum aestivum* L.) and barley (*Hordeum vulgare* L.) plants. Notulae Scientia Biologicae. 2017;9:242-49. <https://doi.org/10.15835/nsb9210075>
24. Faizan M, Rajput VD, Al-Khuraif AA, Arshad M, Minkina T, Sushkova S, Yu F. Effect of foliar fertigation of chitosan nanoparticles on cadmium accumulation and toxicity in *Solanum lycopersicum*. Biology. 2021;10:1-14. <https://doi.org/10.3390/biology10070666>
25. Thakur K, Khurana N, Rani N, Hooda V. Enhanced growth and antioxidant efficiency of *Vigna radiata* seedlings in the presence of titanium dioxide nanoparticles synthesized via the sonochemical method. Israel Journal of Plant Sciences. 2021;69:25-42. <https://doi.org/10.1163/22238980-bja10048>
26. Bradford MM. A rapid and sensitive method for the quantitation of microgram quantities of protein utilizing the principle of protein-dye binding. Analytical Biochemistry. 1976;72:248-54. [https://doi.org/10.1016/0003-2697\(76\)90527-3](https://doi.org/10.1016/0003-2697(76)90527-3)
27. Saharan V, Kumaraswamy RV, Choudhary RC, Kumari S, Pal A, Raliya R, Biswas P. Cu-chitosan nanoparticle mediated sustainable approach to enhance seedling growth in maize by mobilizing reserved food. Journal of Agricultural and Food Chemistry. 2016;64:6148-55. <https://doi.org/10.1021/acs.jafc.6b02239>
28. Kumar M, Turner S. Protocol: A medium-throughput method for determination of cellulose content from single stem pieces of *Arabidopsis thaliana*. Plant Methods. 2015;11:1-8. <https://doi.org/10.1186/s13007-015-0090-6>
29. Dhindsa RS, Plumb-Dhindsa P, Throne TA. Leaf senescence: Correlated with increased levels of membrane permeability and lipid peroxidation and decreased levels of superoxide dismutase and catalase. Journal of Experimental Botany. 1981;32:93-101. <https://doi.org/10.1093/jxb/32.1.93>

30. Rani N, Kumari K, Sangwan P, Barala P, Yadav J, VR, Hooda V. Nano-iron and nano-zinc induced growth and metabolic changes in *Vigna radiata*. *Sustainability*. 2022;14:8251.<https://doi.org/10.3390/su14148251>
31. Nakano Y, Asada K. Hydrogen peroxide is scavenged by ascorbate-specific peroxidase in spinach chloroplasts. *Plant and Cell Physiology*. 1981;22:867-80. <https://doi.org/10.1093/oxfordjournals.pcp.a076232>
32. Thamilarasan V, Sethuraman V, Gopinath K, Balalakshmi C, Govindarajan M, Mothana RA et al. Single step fabrication of chitosan nanocrystals using *Penaeus semisulcatus*: Potential as new insecticides, antimicrobials and plant growth promoters. *Journal of Cluster Science*. 2018;29:375-84. <https://doi.org/10.1007/s10876-018-1342-1>
33. Oh JW, Chun SC, Chandrasekaran M. Preparation and *in vitro* characterization of chitosan nanoparticles and their broad-spectrum antifungal action compared to antibacterial activities against phytopathogens of tomato. *Agronomy*. 2019;9:21. <https://doi.org/10.3390/agronomy9010021>
34. Varma R, Vasudevan S. Extraction, characterization and antimicrobial activity of chitosan from horse mussel, *Modiolus modiolus*. *ACS Omega*. 2020;5:20224-30. <https://doi.org/10.1021/acsomega.0c01903>
35. Chougala LS, Yatnatti MS, Linganagoudar RK, Kamble RR, Kadadevarmath JS. A simple approach on synthesis of TiO₂ nanoparticles and its application in dye-sensitized solar cells. *Journal of Nano and Electronic Physics*. 2017;9:1-6. [10.21272/jnep.9\(4\).04005](https://doi.org/10.21272/jnep.9(4).04005)
36. Grillo R, Rosa AH, Fraceto LF. Engineered nanoparticles and organic matter: A review of the state-of-the-art. *Chemosphere*. 2015;119:608-19. <https://doi.org/10.1016/j.chemosphere.2014.07.049>
37. Divya K, Thampi M, Vijayan S, Shabanamol S, Jisha MS. Chitosan nanoparticles as a rice growth promoter: Evaluation of biological activity. *Archives of Microbiology*. 2022;204:1-11. <https://doi.org/10.1007/s00203-021-02669-w>
38. Navarro E, Baun A, Behra R, Hartmann NB, Filser J, Miao AJ et al. Environmental behavior and ecotoxicity of engineered nanoparticles to algae, plants and fungi. *Ecotoxicology*. 2008;17:372-86. <https://doi.org/10.1007/s10646-008-0214-0>
39. O'Herlihy EA, Duffy EM, Cassells AC. The effects of arbuscular mycorrhizal fungi and chitosan sprays on yield and late blight resistance in potato crops from microplants. *Folia Geobotanica*. 2003;38:201-07. <https://doi.org/10.1007/BF02803152>
40. Ohta K, Atarashi H, Shimatani Y, Matsumoto S, Asao T, Hosoki T. Effects of chitosan with or without nitrogen treatments on seedling growth in *Eustoma grandiflorum* (Raf.) Shinn. Cv. Kairyu Wakamurasaki. *Journal of Japanese Society for Horticulture Science*. 2000;69:63-65. <https://doi.org/10.2503/jjhs.69.63>
41. Behboudi F, Sarvestani TZ, Kassaei MZ, Sanavy SAMM, Sorooshzadeh A, Bidgoli AM. Evaluation of chitosan nanoparticles effects with two application methods on wheat under drought stress. *Journal of Plant Nutrition*. 2019;42:1439-51. <https://doi.org/10.1080/01904167.2019.1617308>
42. Agbodjato NA, Noumavo PA, Adjanohoun A, Agbessi L, Baba-Moussa L. Synergistic effects of plant growth promoting rhizobacteria and chitosan on *in vitro* seeds germination, greenhouse growth and nutrient uptake of maize (*Zea mays* L.). *Biotechnology Research International*. 2016;2016:7830182. <https://doi.org/10.1155/2016/7830182>
43. Van SN, Minh HD, Anh DN. Study on chitosan nanoparticles on biophysical characteristics and growth of *Robusta coffee* in greenhouse. *Biocatalysis and Agricultural Biotechnology*. 2013;2:289-94. <https://doi.org/10.1016/j.bcab.2013.06.001>
44. Ali EF, El-Shehawi AM, Ibrahim OHM, Abdul-Hafeez EY, Moussa MM, Hassan FAS. A vital role of chitosan nanoparticles in improvisation the drought stress tolerance in *Catharanthus roseus* (L.) through biochemical and gene expression modulation. *Plant Physiology and Biochemistry*. 2021;161:166-75. <https://doi.org/10.1016/j.plaphy.2021.02.008>
45. Behboudi F, Sarvestani TZ, Kassaei MZ, Sanavi SAMM, Sorooshzadeh A, Ahmadi SB. Evaluation of chitosan nanoparticles effects on yield and yield components of barley (*Hordeum vulgare* L.) under late season drought stress. *Journal of Water and Environmental Nanotechnology*. 2018;3:22-39. [10.22090/JWENT.2018.01.003](https://doi.org/10.22090/JWENT.2018.01.003)
46. Dowom SA, Karimian Z, Dehnavi MM, Samiei L. Chitosan nanoparticles improve physiological and biochemical responses of *Salvia abrotanoides* (Kar.) under drought stress. *BMC Plant Biology*. 2022;22:364. <https://doi.org/10.1186/s12870-022-03689-4>
47. Samadi N, Yahyaabadi S, Rezayatmand Z. Effect of TiO₂ and TiO₂ nanoparticle on germination, root and shoot length and photosynthetic pigments of *Mentha piperita*. *International Journal of Plant and Soil Sciences*. 2014;3:408-18. <https://doi.org/10.9734/IJPSS/2014/7641>
48. Hawker JS, Marschner H, Downton WJS. Effects of sodium and potassium on starch synthesis in leaves. *Functional Plant Biology*. 1974;1:491-501. <https://doi.org/10.1071/PP9740491>
49. Mohammadi H, Esmailpour M, Gheranpaye A. Effects of TiO₂ nanoparticles and water-deficit stress on morpho-physiological characteristics of dragonhead (*Dracocephalum moldavica* L.) plants. *Acta Agriculturae Slovenica*. 2016;107:385-96. <https://doi.org/10.14720/aas.2016.107.2.11>
50. Jurkow R, Kalisz A, Húška D, Sekara A, Dastborhan S. Sequential changes in antioxidant potential of oakleaf lettuce seedlings caused by nano-TiO₂ treatment. *Nanomaterials*. 2021;11:1171. <https://doi.org/10.3390/nano11051171>